Heterotrophic Archaea dominate sedimentary subsurface ecosystems off Peru

Jennifer F. Biddle[a,b], Julius S. Lipp[b,c], Mark A. Lever[d], Karen G. Lloyd[d], Ketil B. Sørensen[d], Rika Anderson[c,e], Helen F. Fredricks[f], Marcus Elvert[c], Timothy J. Kelly[a,g], Daniel P. Schrag[h], Mitchell L. Sogin[i], Jean E. Brenchley[a,j], Andreas Teske[d], Christopher H. House[a,g], and Kai-Uwe Hinrichs[c,f,k]

[a]Pennsylvania State Astrobiology Research Center and Departments of [g]Geosciences and [j]Biochemistry and Molecular Biology, Pennsylvania State University, University Park, PA 16802; [c]Organic Geochemistry Group, Deutsche Forschungsgemeinschaft Research Center for Ocean Margins and Department of Geosciences, University of Bremen, D-28334 Bremen, Germany; [d]Department of Marine Sciences, University of North Carolina, Chapel Hill, NC 27599; [e]Carleton College, Northfield, MN 55057; [f]Department of Geology and Geophysics, Woods Hole Oceanographic Institution, Woods Hole, MA 02543; [h]Department of Earth and Planetary Sciences, Harvard University, Cambridge, MA 02138; and [i]The Josephine Bay Paul Center for Comparative Molecular Biology and Evolution, Marine Biological Laboratory, Woods Hole, MA 02543

Communicated by John M. Hayes, Woods Hole Oceanographic Institution, Woods Hole, MA, January 5, 2006 (received for review October 22, 2005)

Studies of deeply buried, sedimentary microbial communities and associated biogeochemical processes during Ocean Drilling Program Leg 201 showed elevated prokaryotic cell numbers in sediment layers where methane is consumed anaerobically at the expense of sulfate. Here, we show that extractable archaeal rRNA, selecting only for active community members in these ecosystems, is dominated by sequences of uncultivated Archaea affiliated with the Marine Benthic Group B and the Miscellaneous Crenarchaeotal Group, whereas known methanotrophic Archaea are not detectable. Carbon flow reconstructions based on stable isotopic compositions of whole archaeal cells, intact archaeal membrane lipids, and other sedimentary carbon pools indicate that these Archaea assimilate sedimentary organic compounds other than methane even though methanotrophy accounts for a major fraction of carbon cycled in these ecosystems. Oxidation of methane by members of Marine Benthic Group B and the Miscellaneous Crenarchaeotal Group without assimilation of methane–carbon provides a plausible explanation. Maintenance energies of these subsurface communities appear to be orders of magnitude lower than minimum values known from laboratory observations, and ecosystem-level carbon budgets suggest that community turnover times are on the order of 100–2,000 years. Our study provides clues about the metabolic functionality of two cosmopolitan groups of uncultured Archaea.

anaerobic methanotrophy | deep biosphere | FISH–secondary ion MS | intact polar lipids | stable carbon isotopes

The microbial ecosystem in deeply buried marine sediments may comprise one-tenth of Earth's living biomass (1, 2), but little is known about the organisms, their physiologies, and their influence on surface environments. Geochemical modeling suggests that microbial respiration in marine subsurface sediments is largely dominated by sulfate reduction coupled to the anaerobic oxidation of methane (AOM) (3). In deeply buried sediments, this process is typically observed in a sediment horizon into which both methane and sulfate diffuse, hereafter termed "sulfate-methane transition zone" (SMTZ), and where both compounds are consumed in equimolar amounts (e.g., ref. 4). Our knowledge about the microorganisms mediating AOM is largely based on studies of methane seep environments, where high concentrations of methane and sulfate promote high activities of syntrophic consortia of archaea and bacteria (e.g., ref. 5). Little is known about the microorganisms mediating AOM in diffusive settings with low fluxes of methane and sulfate such as deeply buried SMTZs.

During Ocean Drilling Program (ODP) Leg 201, which targeted sediments underlying highly productive surface waters off Peru, strikingly elevated concentrations of cells were detected by the acridine orange staining technique in three deeply buried SMTZs (6, 7) (see Fig. 4, which is published as supporting information on the PNAS web site). The SMTZs are located at sediment depths of ≈10 m (ODP Site 1230), ≈30 m (Site 1229, top SMTZ), ≈40 m (Site 1227), and ≈88 m (Site 1229, bottom SMTZ) and may have a vertical extension of up to a few meters as indicated by various geochemical parameters (6). Microbial activity in these sediments is indicated by a large variety of geochemical parameters (6, 7), the presence of cultivable Bacteria (7), intact cells, and intact DNA of both Archaea and Bacteria (8–11). These studies suggest that (*i*) a significant fraction of the cells detected with acridine orange is active (11), and (*ii*) a high genetic diversity exists and is somehow linked to geochemical conditions (8, 10), while (*iii*) views of the composition of microbial communities derived from different approaches remain controversial (8–11).

Here, we constrain community composition and processes in deeply buried sediments in and outside SMTZs using a previously undescribed combination of molecular and isotopic techniques that provide insight into the ecosystem's carbon flow regime while selecting for only truly active community members.

Results and Discussion

Archaeal Communities in SMTZs. Extractable archaeal 16S rRNA is an indicator of active subsurface Archaea while excluding inactive cells and fossil DNA (12). In the four SMTZs sampled during ODP Leg 201, 16S rRNA is dominated by sequences belonging to the uncultured Marine Benthic Group B and Miscellaneous Crenarchaeotal Group (Fig. 1; see also Fig. 5, which is published as supporting information on the PNAS web site). Both previously undescribed groups also have been detected by analysis of DNA from the investigated sites (8, 10) and, in fact, are widely distributed throughout marine subsurface environments (13, 14) (A.T., M.A.L., K.G.L., and K.B.S., unpublished data), but their physiologies are unknown. Notably, sequences from methanotrophic Archaea that inhabit surface sediments (15) were not detected in rRNA and also have been absent in DNA libraries (8, 10).

Similar to rRNA, intact polar lipids (IPLs) also are presumed to represent living rather than fossil biomass (16). The IPLs from these sediments are dominated by archaeal glycerol-dialkyl-glycerol-tetraethers (GDGT), followed by glycerol-dialkyl-diether, both types attached to diglycosidic polar headgroups (Fig. 2; see also Table 3, which is published as supporting information on the PNAS

Conflict of interest statement: No conflicts declared.

Abbreviations: AOM, anaerobic oxidation of methane; DIC, dissolved inorganic carbon; IPL, intact polar lipid; ODP, Ocean Drilling Program; OM, organic matter; SMTZ, sulfate-methane transition zone; TOC, total organic carbon.

Data deposition: The sequences reported in this paper have been deposited in the GenBank database (accession nos. DQ302001–DQ302032).

[b]J.F.B. and J.S.L. contributed equally to this work.

[k]To whom correspondence should be addressed at: Organic Geochemistry Group, RCOM and Department of Geosciences, University of Bremen, PO Box 330 440, 28334 Bremen, Germany. E-mail: khinrichs@uni-bremen.de.

 www.pnas.org/cgi/doi/10.1073/pnas.0600035103

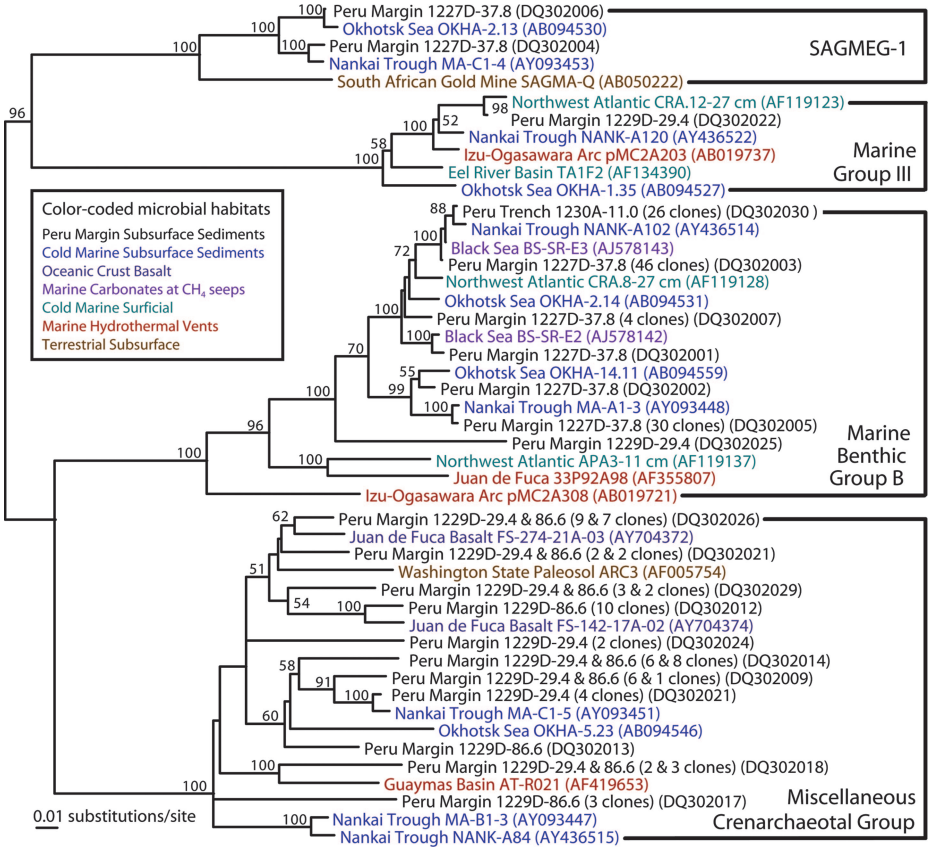

Fig. 1. A 16S rRNA archaeal phylogenetic tree based on maximum likelihood distances of ≈900 nucleotide positions (16S rRNA positions 23–914). Bootstrap numbers are based on 200 resamplings. Sequences were obtained from four sediment samples from each of the four SMTZs encountered during ODP Leg 201: 1227D-37.8 (ODP Hole-depth in hole in meters below seafloor), 1229D-29.4, 1229D-86.8, and 1230A-11.0. Closely related sequence clusters are represented by single sequences, annotated with the number of near-identical 16S rRNA clones that they represent and their GenBank accession numbers. Sequences are color coded by habitat to illustrate the diverse environmental range of these uncultured archaeal lineages.

web site). The presence of calditol-based IPLs (16) and crenarchaeol-derived alkyl chains (17) (Fig. 2) are indicators of crenarchaeotal community members, in agreement with rRNA results. Counts of cells hybridized to a domain-specific archaeal fluorescent *in situ* hybridization (FISH) probe (Fig. 2) offer independent evidence in support of a sizeable and active archaeal community. As with the extraction of rRNA and IPLs, the FISH protocols applied in our study are considered to select for active members of the population.

Both counts of FISH-labeled Bacteria and Archaea and relative distributions of IPLs (Table 1) suggest that the active portion of the microbial community is dominated by Archaea. At all sites, the highest relative abundance of Archaea is found within SMTZs. The situation is not much different outside SMTZs; only two samples from 0.7 m below seafloor at Sites 1227 and 1229 showed slightly higher bacterial than archaeal counts (Table 1). Similarly, bacterial IPLs were not identified in any of the analyzed samples. Unidentified compounds present in some samples do not show any of the mass spectrometric properties observed during analysis of a large variety of bacterial IPLs in both environmental samples and cultures of environmentally relevant bacteria (K.-U.H., H.F.F., J.S.L., F. Schubotz, and T. Mohr, unpublished data) and are considered unlikely to be of bacterial origin. In SMTZs at Sites 1227 and 1229, archaeal cells account for at least 80% of total hybridized Archaea and Bacteria, whereas at Site 1230 the archaeal proportion is at ≈60%, somewhat lower. The highest concentrations of archaeal cells, up to 6×10^6 cells per cm^{-3} sediment, were found at the two SMTZs at Site 1229, followed by Site 1230 (Table 1). The relative abundance of archaeal lipids also peaks at the two SMTZs of Site 1229 (Table 1). Notably, relative yields of archaeal rRNA determined throughout the sediment column at Site 1227 were ≈2 orders of magnitude higher in the SMTZ than outside, suggestive of a drastic increase of active archaea (K.B.S. and A.T., unpublished data).

Support for an important role of Archaea in subsurface sediments off Peru comes from a study of Site 1229 by Mauclaire *et al.* (9), who counted archaeal cells directly with catalyzed reporter deposition (CARD)-FISH, a technique shown to increase the sensitivity for detecting moderately active cells (18). Conversely, Schippers *et al.* (11) inferred from quantitative PCR that DNA extracts from sediments at Sites 1227 and 1230, including those from SMTZs, are dominated by Bacteria, whereas archaeal cell estimates are 10^5 ml^{-1} and lower. In the same study, CARD-FISH did not detect Archaea in amounts sufficient for direct counts (11). These conflicting data stress that distinguishing between presence and activity of subsurface prokaryotes remains a major problem.

Isotopic Constraints on the Carbon Metabolism of Subsurface Archaeal Communities. The profiles of $\delta^{13}C$ of dissolved inorganic carbon (DIC) exhibit minima in SMTZs (profiles not shown) and suggest production of DIC by AOM. $\delta^{13}C$ of archaeal biomass depends on the $\delta^{13}C$ of the substrates used for cell growth and/or the carbon fixation pathway (e.g., ref. 19). Because of strong ^{13}C-depletions commonly observed in methane, the biomass of methane-oxidizing Archaea is typically strongly depleted in ^{13}C (e.g., ref. 20). $\delta^{13}C$ of deeply buried Archaea was determined by two independent techniques in adjacent samples, i.e., on whole cells by FISH coupled to secondary ion mass spectrometry (SIMS) (cf. ref. 21) and by compound-specific analyses of IPLs. The $\delta^{13}C$ values of archaeal cells and IPLs in SMTZs are uniform and average at −20‰ ($n = 8$ samples; 98 cells total) and −24‰ ($n = 8$ samples; expressed as weighted average of δ values obtained for hydrocarbon derivatives prepared from IPLs), respectively, and are not significantly different from values obtained for archaeal biomass in sediments above the SMTZ (Fig. 3).

We draw the following conclusions from the isotopic relationships between archaeal biomass and other sedimentary carbon pools (Fig. 3). (*i*) Given the consistently high ^{13}C-depletion in

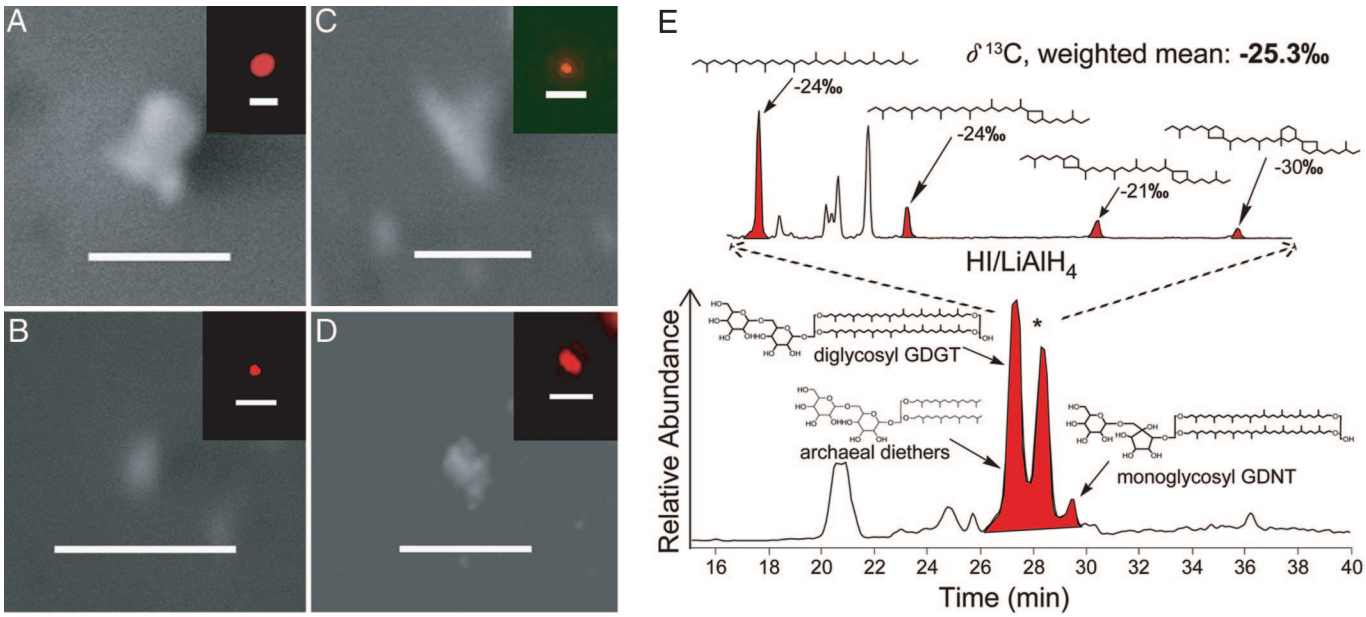

Fig. 2. Microscopic images of archaeal cells (*A–D*) and chromatograms of gas and liquid chromatographic analyses of archaeal lipids (*E*). (*A–D*) Environmental scanning electron microscopy (ESEM) images of individual cell targets in the following samples: 1227D-34.4 (*A*) (ODP Hole-depth in hole in meters below seafloor), 1229D-29.8 (*B*), 1229D-86.8 (*C*), and 1230C-9.1 (*D*). (Scale bars: 1 μm.) *Insets* show FISH images of the same cells. All ESEM analyses showed small cells, most <1 μm in diameter. All images have been subjected to postexposure software enhancement to increase brightness and contrast. (*E Lower*) Positive ion base-peak HPLC-MS chromatogram of a fraction resulting from consecutive trapping of archaeal IPLs by preparative HPLC-MS of sample 1229D-87.1. Red labeled peaks designate archaeal glycerol-dialkyl-glycerol-tetraethers (GDGTs) with smaller quantities of coeluting archaeal glyceroldialkylethers (structures shown; *, tentatively identified as GDGT derivative). (*Upper*) Total ion current GC-MS chromatogram of isoprenoid hydrocarbons released from IPLs by ether cleavage and subsequent reduction (δ^{13}C of individual compounds is reported in Table 3).

methane, the δ values of archaeal biomass indicate that only a small fraction, if any, of the archaeal populations relies on methane as carbon source. (*ii*) The relatively small ^{13}C-depletion of archaeal biomass relative to DIC indicates that autotrophic processes such as methanogenesis via CO_2 reduction are not fueling the bulk of the archaeal communities (22). (*iii*) The small ^{13}C-depletion of lipids relative to bulk biomass eliminates an important role of methylotrophic methanogens (23). (*iv*) Instead, the similarity of isotopic compositions of archaeal biomass and total organic carbon (TOC) is striking and suggests that the bulk archaeal community assimilates organic compounds derived from fossil organic matter (OM). The variability of isotopic compositions of both hydrocarbon derivatives prepared from IPLs (Table 3) and individual archaeal cells (see Table 4, which is published as supporting information on the PNAS web site) is consistent with some versatility of metabolic reactions and/or carbon sources used by community members, but no single isotopic value points strongly toward assimilation of methane-derived carbon.

Degradation of sedimentary OM probably provides a substantial fraction of carbon for the archaeal community. Likely intermediates are low-molecular-weight organic compounds such as acetate and formate, which are present in all Leg 201 sediments and exhibit elevated concentrations at the SMTZs of Site 1229 (6).

Energy Fluxes and Maintenance Energies. Conceptually, we consider AOM and slow degradation of refractory sedimentary OM as the two principal sources of energy for communities in SMTZs. Electron donors that are independent of photosynthetically produced OM and relevant in other subsurface settings are not important in the Peru Margin subsurface, e.g., H_2 and O_2 from radiolysis of water (24, 25) or H_2 from rock–water reactions (26). Anaerobic degradation of sedimentary OM is typically accomplished by complex syntrophic associations and involves fermentative breakdown of large organic molecules and subsequent reaction of products to CH_4 and CO_2 or, when coupled to sulfate reduction, only to CO_2. Methane fluxes, determined from methane concentration profiles, account for 8% (1229, top SMTZ), 33% (Site 1230), 43% (1229, bottom SMTZ), and 114% (Site 1227) of sulfate fluxes (Table 2). Although loss of methane gas during sample retrieval from high-pressure environments could lead to underestimation of fluxes of methane relative to those of sulfate, alternative sinks of sulfate such as organotrophic sulfate reduction could explain the differences of fluxes of methane and sulfate at the SMTZs at Sites 1229 and 1230. If organotrophic sulfate reduction were performed by archaea and their growth efficiencies were not vastly higher than those of presumed archaeal methanotrophs, the excess in sulfate fluxes over those of methane is not large enough to wipe out an isotopic signature of methane assimilation in all except the upper SMTZ at Site 1229.

The rates of the biologically mediated "basal" degradation of sedimentary OM in SMTZs were estimated on the basis of a diagenetic model (28) that describes the decrease in reactivity with age of the OM (Table 2). The resulting rates are lower than (Sites 1227 and 1230) to approximately equal to (Site 1229) modeled rates of methane turnover in SMTZs (Table 2). Gibbs free-energy changes (ΔG_R) in SMTZs were estimated from turnover rates of both methane and sedimentary organic carbon, and energies to maintain the observed microbial populations were computed by using an empirical model that simulates minimum values known from laboratory cultures (30). The results show that the ΔG_R estimates can only account for a small fraction of the energy that would be required for maintaining the observed communities (Table 2).

Two principal conclusions can be drawn from the energetic considerations: (*i*) Real maintenance energies in subsurface environments must be much lower than what has been experimentally determined in laboratory cultures (e.g., refs. 30 and 31), and (*ii*) AOM is a principal source of metabolic energy in SMTZs. Explanations follow.

(*i*) Multiple lines of evidence suggest the presence of $>10^6$ active

Table 1. Quantification of active archaeal cells hybridized with archaeal FISH probe Arch915-Cy3, percentage archaea of total prokaryotes, and relative quantities of archaeal IPLs

Sample, (core-depth, mbsf)	Archaeal cells, $\times 10^6$ cm^{-3} sed.	Archaea, %	Archaeal IPLs, relative, %
1227D-0.7	9.7 ± 0.11	35	
1227D-34.5	1.3 ± 0.15	96	
1227A-37.6*			48 ± 6
1227D-38.0*	1.5 ± 0.01	98	
1227D-38.2*			39 ± 4
1227A-40.5*	1.7 ± 0.08	98	
1227A-40.9*			31 ± 5
1229D-0.7	2.8 ± 0.40	45	
1229D-1.4			10
1229D-4.3	5.4 ± 0.20	68	
1229D-12.9	9.2 ± 1.61	69	
1229D-29.7*			80 ± 6
1229D-29.8*	6.3 ± 1.13	80	
1229D-30.4*	5.9 ± 0.98	86	
1229D-32.4*			22
1229D-49.8	1 ± 0.17	81	
1229D-49.9			20
1229D-54.3	3.2 ± 0.31	67	
1229D-86.8*	3.2 ± 0.35	94	
1229D-87.1*			100 ± 9
1229D-89.1*	6.4 ± 1.59	98	
1229A-121.1			14
1229A-121.4	1.5 ± 0.37	63	
1230A-0.8			4
1230A-1.3	1.7 ± 0.44	54	
1230C-9.1*	4.3 ± 2.0	63	
1230B-9.7*			17 ± 1
1230B-10.1*			14 ± 2
1230C-10.3*	3.1 ± 0.1	61	
1230C-10.7*	2.9 ± 0.36	56	
Average	2.9	82	34

Percentage archaea of total prokaryotes is based on cells hybridized with probes Arch915-Cy3 and EUB338-FITC. Relative quantities of archaeal IPLs were normalized to the sample with maximum concentration, 1229D-87.1. Values are ±SD of three replicates. mbsf, m below seafloor; sed, sediment. *Samples from SMTZs.

prokaryotic cells per cm^3 of sediment (Table 1), but sedimentary biogeochemical processes can only account for 0.1–2% of the population if conventional maintenance energy requirements are applicable. Conceptually, cellular maintenance energies are probably lower in dormant cells (33), which may be abundant in the deep subsurface. In fact, a dormant fraction of subsurface cells provides one possible explanation for our estimates of long turnover times of subsurface populations (Table 2). Isotopic data indicate that the bulk of the carbon assimilated by subsurface communities is derived from sedimentary OM. With estimated degradation rates in SMTZs ranging from 0.1 to 2.9 $\times$ 10^{-9} mol C·cm^{-3}·yr^{-1}, and a range of growth efficiencies of 0.01–0.06 (31, 32), we derive a range of turnover times for the population of 70–2,150 years (Table 2). Turnover of microbial communities in SMTZs is likely faster than outside where lower total ΔG_R related to the absence of AOM could conceivably result in lower growth efficiencies (cf. ref. 32). Such a vertical distribution of turnover times could provide an explanation for the great excess of cells in SMTZs that are observed by acridine orange staining (cf. Fig. 4) but do not hybridize to FISH probes, i.e., "recently" active cells that have not been degraded yet.

(*ii*) The high fraction of total ΔG_R in SMTZs accounted for by AOM (Table 2), combined with the lack of ^{13}C-depletion in archaeal biomass (Fig. 3), suggests that members of the Marine Benthic Group B and/or Miscellaneous Crenarchaeotal Group Archaea oxidize methane but do not assimilate its carbon. Such "dissimilatory" methane-oxidizing process could account for our observations and would resemble metabolic strategies found in other Archaea. For example, several CO_2-reducing methanogens use auxiliary carbon substrates and complex organic nutrients for synthesis of cell material and growth, while CO_2 is converted into methane (34, 35).

Marine Benthic Group B and Miscellaneous Crenarchaeotal Group Archaea, presumably dominant members in subsurface ecosystems, have cosmopolitan distributions in a wide range of biogeochemically distinct sedimentary settings (Figs. 1 and 5), suggestive of a considerable ecophysiological flexibility. More widespread and improved quantifications may show that these subsurface Archaea, in analogy to planktonic Marine Group I Archaea in the ocean (36), constitute a significant fraction of the prokaryotic biomass in Earth's subsurface. Our insights into carbon sources of these uncultured Archaea may form essential building blocks toward understanding the microbial carbon cycle in deep marine sediments.

Materials and Methods

Sample Collection. All samples were collected on ODP Leg 201 at Sites 1227, 1229, and 1230 (6). Whole round cores frozen at −80°C were used for lipid and RNA studies. Fixed sediment was used for FISH studies (6).

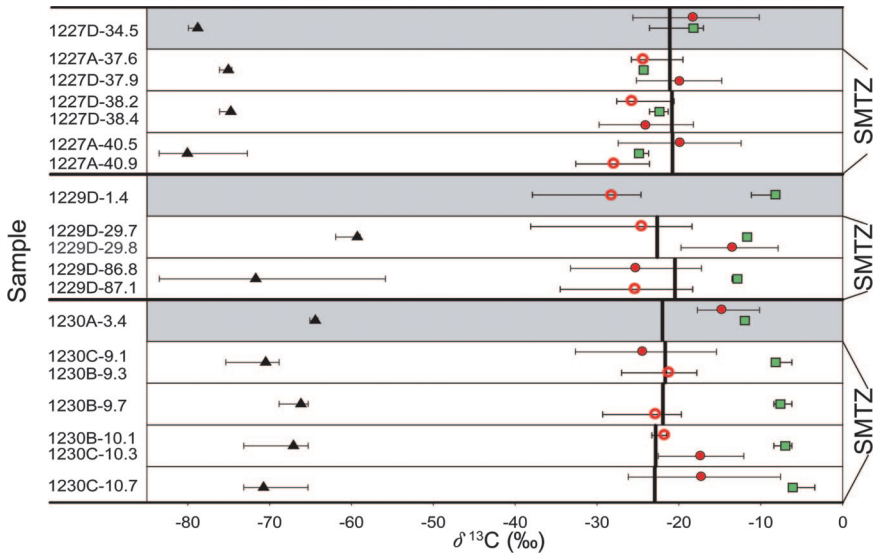

Fig. 3. δ^{13}C values of sedimentary methane (filled triangles; linearly interpolated from sample depth used for gas analysis to depth of samples used for FISH and IPL analysis; endpoints of bars indicate actual δ values of methane), DIC (green squares; linearly interpolated, as above), archaeal cells determined by FISH–secondary ion MS (filled red circles; weighted mean of all samples for each site; bars show the error on that mean; mean squares weighted deviation ranges were 0.1–1.5), and archaeal IPLs (open red circles; circle shows the weighted mean δ^{13}C of all IPL-derived archaeal hydrocarbons; line shows the range of individual compounds). Brown bars designate δ^{13}C of TOC. Gray-shaded samples stem from sediments above the SMTZ. Sample names: ODP Hole-depth in hole in meters below seafloor.

Table 2. Average values of total hybridized cells, fluxes, rates of AOM and OC degradation, and related ΔG_R, energies required to maintain the observed populations, and community turnover times in SMTZs

Site; SMTZ	Hybridized cells*	CH_4 flux into SMTZ†	SO_4^{2-} flux into SMTZ†	AOM rate‡	OC degradation rate§	ΔG_R, AOM¶	ΔG_R, OC degradation‖	Maintenance energy**	Turnover time,†† years
1227	1.6	0.16	0.14	1.6	0.1	27	2.8/4.7	15,000	360/2150
1229T	7.4	0.08	0.95	0.8	2.9	14	67/114	71,000	70/410
1229B	5.0	0.13	0.30	1.3	1.1	15	27/46	55,000	120/690
1230	6.7	0.88	2.58	8.8	1.7	114	39/66	20,000	110/640

Additional information on the calculations is provided in *Supporting Text*.

*Total hybridized cells with probes Arch915-Cy3 and EUB338-FITC (Table 1). Values are $\times 10^6$ cm^{-3}.

†Fluxes were calculated from pore water concentrations and physical property data (6) according to Schulz (27). Only the linear parts of methane and sulfate gradients into SMTZs were considered. Values are $\times 10^{-6}$ $mol \cdot cm^{-2} \cdot yr^{-1}$.

‡Estimated from fluxes of methane, assuming a vertical extension of the reactive zone of the SMTZ of 100 cm. Values are $\times 10^{-9}$ $mol \cdot cm^{-3} \cdot yr^{-1}$.

§Based on the diagenetic model by Middelburg (ref. 28; see text for details). Values are $\times 10^{-9}$ $mol \cdot cm^{-3} \cdot yr^{-1}$.

¶Using a ΔG_R for AOM of -17.2 $kJ \cdot mol^{-1}$ (1227); -16.9 $kJ \cdot mol^{-1}$ (1229T); -11.9 $kJ \cdot mol^{-1}$ (1229B), and -12.9 $kJ \cdot mol^{-1}$ (1230). Values are $\times 10^{-6}$ $J \cdot cm^{-3} \cdot yr^{-1}$.

‖Calculated using hexadecane as model compound for sedimentary OM (15); assumes ΔG_R of syntrophic breakdown under methanogenic (-23.4 $kJ \cdot mol^{-1}$ C; first value) and sulfate-reducing conditions (-40 $kJ \cdot mol^{-1}$ C; second value) (29). Values are $\times 10^{-6}$ $J \cdot cm^{-3} \cdot yr^{-1}$.

**Based on a calculation of temperature-dependent, species-independent maintenance energies (30). The cellular maintenance energies resulting from this model are close to the lowest known values determined experimentally for anaerobic bacteria (*Acetobacterium woodii* grown on lactate; ref. 31). Values are $\times 10^{-6}$ $J \cdot cm^{-3} \cdot yr^{-1}$.

††Based on total amount of carbon in the population of hybridized cells and OC degradation rate in combination with growth efficiencies of 0.01 (32) (higher value; planktonic heterotrophic bacteria in highly oligotrophic ocean) to 0.06 (31) (lower value; maximum value found for syntrophic propionate-degrading community).

FISH Analysis. Fixed samples kept at −20°C were diluted in 1× PBS and spotted on 1-inch glass rounds and 10-welled slides. Dried samples were subjected to traditional FISH (21) by using the standard probes ARCH915-CY3 (37) and EUB338-FITC (38). Slides were dehydrated in a series of ethanol baths (55%, 85%, 95%; 3 min each), then covered with 10 μl of hybridization buffer (22) (20% formamide, pH 8.0/40 ng of each probe). Slides were incubated in a premoistened hybridization chamber for 90 min at 46°C, then washed for 15 min at 48°C (21) and viewed with a Nikon E800 microscope. Because both archaeal and bacterial probes were used at the same time in experiments, the digital overlay of the two fluorochrome images served to identify nonspecific binding of probes, and only cells illuminated by one fluorochrome were counted. Exposure times of 0.5–5 s were needed to capture cell fluorescence, and only single cells were observed. Counts are based on a total of 400 cells counted per horizon, viewed in random fields. Error is reported as the standard deviation of three replicate counts on each sample. Separately, both CY3 and FITC NON probes were used; however, the amount of nonspecific binding was not significant compared with the estimated error of the counts. The reversal of probe fluorochromes produced similar results (data not shown). Additional controls were run by using pure cultures of microbes with and without added sediment. Samples on 1-inch glass rounds had the location of cells recorded and documented with a series of phase contrast and epifluorescent images using 10×, 40×, 60×, and 100× dry objectives on a Nikon E800. PHOTOSHOP software (Adobe Systems, San Jose, CA) was used to enhance and organize these images into digital maps of each slide. Targets were then located on a FEI Quanta 200 Environmental Scanning Electron Microscope (Penn State, Materials Resource Institute) to ensure that individual cells were separated from other material. Rounds were subsequently gold coated and used for microprobe analysis.

Isotopic Compositions of Whole Cells by Secondary Ion MS Analysis. The carbon isotopic composition of individual target cells was analyzed on the IMS 1270 (Cameca, Paris) at the Ion Microprobe Facility at the University of California, Los Angeles. Secondary C_2^- ions were sputtered by a 10-μm-diameter Cs^+ beam from the target biomass and analyzed in monocollection mode by using the electron multiplier with a field aperture of 5 μm^2. Instrumental mass fractionation was calibrated by the comparison of *Escherichia coli* cells measured by ion microprobe and by elemental analyzer-MS, and data were appropriately corrected (data not shown). Data of individual cells, resulting weighted means of all cells, the errors on that mean, and the mean squared weighted deviations are reported in Table 4.

Extraction and Separation of Lipids. Fifty grams of dry sediment were spiked with an internal standard (1-*O*-hexadecyl-2-acetoyl-*sn*-glycero-3-phosphocholine; PAF) and extracted by a modified Bligh and Dyer method in four steps (16) followed by 10-min centrifugation at 800 × *g*. The combined supernatants were washed with water and evaporated to dryness. The total lipid extract was separated chromatographically in two fractions on a glass column (4 g of silica gel, 60 Mesh; nonpolar fraction, 20 ml of dichloromethane; polar fraction containing glycolipids and phospholipids, 20 ml of acetone followed by 40 ml of methanol).

HPLC-MS Analysis of IPLs. HPLC-MS analysis was performed at the University of Bremen. Details are provided in ref. 16. Relative concentrations of IPLs for intersample comparison were calculated based on MS response of molecular ions relative to that of known amounts of the internal standard. Lack of authentic standards prevented determination of absolute concentrations because response factors of different IPLs vary significantly. IPL concentrations (roughly estimated in the lower ng/g sediment-range) were too low for detection with an evaporative-light-scattering detector.

Preparation of IPL Derivatives for Isotopic Analysis. Stable carbon isotopic compositions, $\delta^{13}C$, were determined on isopranyl derivatives prepared from archaeal IPLs by ether cleavage with HI and subsequent reduction with $LiAlH_4$ (e.g., ref. 39). To avoid incorporation of ether-bound alkyl moieties that may be present in polar, high-molecular-weight organic material, we collected archaeal IPLs during 10 repeated injections on a wide-bore preparative HPLC column (LiChrosphere Si60, 5 μm, 250 × 10 mm; Alltech Associates) with a fraction collector. The flow rate was 1.5 ml/min, and the solvent gradient was 100% A to 100% B in 120 min, hold for 30 min followed by 90 min reequilibration with 100% A; eluents were as in ref. 16.

MS and Isotopic Analysis of IPL Derivatives. Products released from archaeal IPLs were identified and quantified on a Trace GC-MS (ThermoFinnigan, San Jose, CA). The GC was operated at 310°C in split/splitless mode and equipped with a Varian VF5-ms capillary column (L = 30 m; ID = 0.25 mm; 0.25 μm film thickness; He as carrier gas; flow = 1 ml/min). The column temperature was programmed from 60°C (1 min) at 10°C/min to 150°C followed by

4°C/min to 310°C (25 min). Compound-specific isotope analyses of IPL derivatives were performed on a Hewlett–Packard 5890 GC equipped with an on column injector and an IVA OV-1 capillary column (L = 60 m; ID = 0.32 mm; 0.25-μm film thickness). The column temperature was programmed from 60°C (1 min) at 10°C/min to 150°C followed by 4°C/min to 310°C (30 min). The GC was coupled via a combustion interface (set at 940°C) to a MAT252 isotope-ratio-monitoring mass spectrometer (ThermoFinnigan).

Isotopic Analysis of Methane, TOC, and DIC. δ^{13}C of methane, TOC, and DIC was determined by using standard protocols. Details are provided in *Supporting Text*, which is published as supporting information on the PNAS web site.

Ribosomal RNA Extraction, Reverse Transcription, Cloning, and Sequencing. RNA was extracted from the center of whole-round core samples 1227D-37.8, 1229D-29.7, 1229D-86.8, and 1230A-11.1. Following a modification of published protocols (40, 41), a volume of 4 ml sediment was mixed with 5 ml of phenol (pH 5), 5 ml of 5× extraction buffer (250 mM NaAc/50 mM EDTA, pH 5), and 0.5 ml of 20% SDS, distributed over 2-ml bead beating tubes with 0.5 g of 0.1-mm zirconium beads (Biospec Products, Bartlesville, OK), homogenized for 30 s at level 6.5 on a FastPrep FP120 homogenizer (Qbiogene, Carlsbad, CA), and centrifuged (5 min; 16,000 × *g*; 4°C). Aqueous phases were removed and saved. The remaining phenol and sediment pellets were homogenized and extracted once more using 300 μl of 1× extraction buffer. The combined aqueous phases were extracted in phenol, 1:1 phenol/chloroform, and chloroform by vortexing and centrifugation. RNA was precipitated for 2 h at −20°C in 0.5 vol of 7.5 M ammonium acetate and 1 vol of isopropanol. Precipitates were washed in 70% ethanol, air dried, and resuspended in 90 μl of water. Each extraction product was incubated with 10 μl of DNAse buffer and 4 μl of DNAse (Fisher) for 30 min at 37°C and purified (RNeasy Mini Kit; Qiagen, Valencia, CA). Negative controls were run as parallel extractions without sediment.

The RNA was reverse transcribed and amplified with primers 8f (42) and 915r (43) by using the One-Step RT-PCR kit (Qiagen) and the following PCR protocol: (*i*) 30-min reverse transcription at 50°C, (*ii*) 15-min *Taq* polymerase activation at 95°C, (*iii*) 40 cycles of 30–45 s denaturation at 92–94°C, 30–45 s annealing at 58°C, 4 min amplification at 72°C, and (*iv*) a final amplification step of 6–10 min. RT-PCR products were checked by gel electrophoresis on 1.5% agarose gels. PCR assays without the reverse transcription step showed the absence of DNA contamination.

RT-PCR products were cloned with the TOPO XL PCR cloning kit (Invitrogen) according to the manufacturer's instructions. Plasmid extraction, purification and cycle sequencing was performed at the Marine Biological Laboratory (Woods Hole, MA). Sequences were BLAST analyzed against GenBank (www.ncbi.nlm.nih.gov/blast) and screened for chimeras with the CHECK_CHIMERA application (Ribosomal Database Project, http://geta.life.uiuc.edu/RDP/commands/chimera.html) and by constructing phylogenetic trees from sequence fragments (base pairs 1–250, 251–500, 501–end). Sequences were aligned in ARB (www.arb-home.de), and alignments were edited in SEQPUP (Version 0.6, http://iubio.bio.indiana.edu/soft/molbio/seqpup/java/seqpup-doc.html). Phylogenetic trees (maximum likelihood distance) and bootstrap analyses (200 replicates) were performed in PAUP4.0* (Sinauer Associates, Sunderland, MA).

We thank the ODP Leg 201 Shipboard Scientific Party for sample recovery and data; C. G. Johnson, H. Buschhoff, and M. Segl for technical support during isotopic analysis of methane and TOC; and J. M. Hayes, A. Schippers, and two anonymous reviewers for constructive comments that improved this manuscript. Samples for this research were provided by ODP [sponsored by the National Science Foundation (NSF) and participating countries under the Joint Oceanographic Institutions]. This work was supported by Deutsche Forschungsgemeinschaft (to J.S.L., R.A., M.E., and K.-U.H. at Research Center for Ocean Margins and Grant Hi 616/4 to K.U.-H.); National Aeronautics and Space Administration Astrobiology Institute Grants NNA04CC06A (to J.E.B. and C.H.H. at Pennsylvania State University), NCC 2-1275 (to M.A.L., K.G.L., K.B.S., H.F.F., A.T., and K.-U.H. at the University of Rhode Island), and NCC 2-1054 (to M.L.S. and A.T. at the Marine Biological Laboratory); the G. Unger Vetlesen Foundation; U.S. Department of Energy Grant DE-FG02-93ER20117; and NSF Grant MCB03-48492. J.F.B. was supported by NSF Integrative Graduate Education and Research Traineeship Program Grant DGE-9972759 and a Schlanger fellowship from the Joint Oceanographic Institutions (JOI). M.A.L. was supported in part by postcruise support from JOI. The University of California, Los Angeles ion microprobe is supported by the W. M. Keck Foundation and NSF Grant EAR 01-13563. This work is Research Center for Ocean Margins Publication No. 359.

1. Parkes, R. J., Cragg, B. A. & Wellsbury, P. (2000) *Hydrogeol. J.* **8,** 11–28.
2. Whitman, W. B., Coleman, D. C. & Wiebe, W. J. (1998) *Proc. Natl. Acad. Sci. USA* **95,** 6578–6583.
3. D'Hondt, S., Rutherford, S. & Spivack, A. J. (2002) *Science* **295,** 2067–2070.
4. Iversen, N. & Jørgensen, B. B. (1985) *Limnol. Oceanogr.* **30,** 944–955.
5. Hinrichs, K.-U. & Boetius, A. (2002) in *Ocean Margin Systems*, eds. Wefer G., Billet, D., Hebbeln, D., Jørgensen, B. B., Schlüter, M. & van Weering, T. (Springer, Berlin), pp. 457–477.
6. D'Hondt, S. L., Jørgensen, B. B., Miller, D. J. & Shipboard Scientific Party (2003) *Proceedings of the Ocean Drilling Program: Initial Reports* (Ocean Drilling Program, Texas A & M University, College Station, TX), Vol. 201.
7. D'Hondt, S. L., Jørgensen, B. B., Miller, D. J., Batzke, A., Blake, R., Cragg, B. A., Cypionka, H., Dickens, G. R., Ferdelman, T., Hinrichs, K.-U., *et al.* (2004) *Science* **306**, 2216–2221.
8. Inagaki, F., Nunoura, T., Nakagawa, S., Teske, A., Lever, M., Lauer, A., Suzuki, M., Takai, K., Delwiche, M., Colwell, F. S., *et al.* (2006) *Proc. Natl. Acad. Sci. USA* **103,** 2815–2820.
9. Mauclaire, L., Zepp, K., Meister, P. & McKenzie, J. (2005) *Geobiology* **2,** 217–223.
10. Parkes, R. J., Webster, G., Cragg, B. A., Weightman, A. J., Newberry, C. J., Ferdelman, T. G., Kallmeyer, J., Jørgensen, B. B., Aiello, I., W. & Fry, J. C. (2005) *Nature* **436**, 390–394.
11. Schippers, A., Neretin, L. N., Kallmeyer, J., Ferdelman, T. G., Cragg, B. A., Parkes, R. J. & Jørgensen, B. B. (2005) *Nature* **433**, 861–864 .
12. Inagaki, F., Okada, H., Tsapin, A. I. & Nealson, K. H. (2005) *Astrobiology* **5,** 141–153.
13. Inagaki, F., Suzuki, M., Takai, K., Oida, H., Sakamoto, T., Aoki, K., Nealson, K. H. & Horikoshi, K. (2003) *Appl. Environ. Microbiol.* **69,** 7224–7235.
14. Coolen, M. J. L., Cypionka, H., Sass, H. & Overmann, J. (2002) *Science* **296,** 2407–2410.
15. Orphan, V. J., Hinrichs, K.-U., Ussler, W., III, Paull, C. K., Taylor, L. T., Sylva, S. P., Hayes, J. M. & Delong, E. F. (2001) *Appl. Environ. Microbiol.* **67,** 1922–1934.
16. Sturt, H. F., Summons, R. E., Smith, K., Elvert, M. & Hinrichs, K.-U. (2004) *Rapid Commun. Mass Spectrom.* **18,** 617–628.
17. Sinninghe Damsté, J. S., Schouten, S., Hopmans, E. C., Van Duin, A. C. T. & Geenevasen, J. A. J. (2002) *J. Lipid Res.* **43,** 1641–1651.
18. Amann, R. I., Zarda, B., Stahl, D. A. & Schleifer, K. (1992) *Appl. Environ. Microbiol.* **58,** 3007–3011.
19. Hayes, J. M. (2001) *Rev. Mineral. Geochem.* **43,** 1–31.
20. Hinrichs, K.-U., Hayes, J. M., Sylva, S. P., Brewer, P. G. & DeLong, E. F. (1999) *Nature* **398,** 802–805.
21. Orphan, V. J., House, C. H., Hinrichs, K.-U., McKeegan, K. D. & DeLong, E. F. (2001) *Science* **293,** 484–487.
22. House, C. H., Schopf, J. W. & Stetter, K. O. (2003) *Org. Geochem.* **34,** 345–356.
23. Summons, R. E., Franzmann, P. D. & Nichols, P. D. (1998) *Org. Geochem.* **28,** 465–476.
24. Lin, L.-H., Hall, J, Lippmann-Pipke, J., Ward, J. A., Sherwood Lollar, B., DeFlaun, M., Rothmel, R., Moser, D., Gihring, T. M., Mislowack, B., *et al.* (2005), *Geochem. Geophys. Geosyst.* **6,** Q07003.
25. Blair, C., D'Hondt, S. & Spivack, A. J. (2005) *Astrobiology* **5,** 250.
26. Stevens, T. O. & McKinley, J. P. (1995) *Science* **270,** 450–454.
27. Schulz, H. D. (2000) in *Marine Geochemistry*, eds. Schulz, H. D. & Zabel, M. (Springer, Berlin), pp. 85–128.
28. Middelburg, J. J. (1989) *Geochim. Cosmochim. Acta* **53,** 1577–1581.
29. Zengler, K., Richnow, H. H., Rossello-Mora, R., Michaelis, W. & Widdel, F. (1999) *Nature* **401,** 266–269.
30. Tijhuis, L., Van Loosdrecht, M. C. M. & Heijnen, J. J. (1993) *Biotechnol. Bioeng.* **42,** 509–519.
31. Scholten, J. C. M. & Conrad, R. (2000) *Appl. Environ. Microbiol.* **66,** 2934–2942.
32. del Giorgio, P. A. & Cole, J. J. (1998) *Ann. Rev. Ecol. Syst.* **29,** 503–541.
33. Harder, J. (1997) *FEMS Microbiol. Ecol.* **23,** 39–44.
34. Boone, D. R., Whitman, W. B. & Koga, Y. (2001) in *Bergey's Manual of Systematic Bacteriology*, eds. Boone, D. R. & Castenholz, R. W. (Springer, New York), Vol. 1, pp. 246–267.
35. Boone, D. R., Whitman, W. B. & Koga, Y. (2001) in *Bergey's Manual of Systematic Bacteriology*, eds. Boone, D. R. & Castenholz, R. W. (Springer, New York), Vol. 1, pp. 268–294.
36. Karner, M. B., DeLong, E. F. & Karl, D. M. (2001) *Nature* **409,** 507–510.
37. Amann, R. I., Binder, B. J., Olson, A. J., Chisholm, S. W., Devereux, R. & Stahl, D. A. (1990) *Appl. Environ. Microbiol.* **56,** 1919–1925.
38. Stahl, D. A. & Amann, R. (1991) in *Sequencing and Hybridization Techniques in Bacterial Systematics*, eds. Stackebrandt, E. & Goodfellow, M. (Wiley, Chichester, U.K.), pp. 205–248.
39. DeLong, E. F., King, L. L., Massana, R., Cittone, H., Murray, A. E., Schleper, C. & Wakeham, S. G. (1998) *Appl. Environ. Microbiol.* **64,** 1133–1138.
40. MacGregor, B. J., Moser, D. P., Alm, E. W., Nealson, K. H. & Stahl, D. A. (1997) *Appl. Environ. Microbiol.* **63,** 1178–1181.
41. Stahl, D. A., Flesher, B., Mansfield, H. R. & Montgomery L. (1988) *Appl. Environ. Microbiol.* **54,** 1079–1084.
42. Teske, A., Hinrichs, K.-U., Edgcomb, V., de Vera Gomez, A., Kysela, D., Sylva, S. P., Sogin, M. L. & Jannasch, H. W. (2002) *Appl. Environ. Microbiol.* **68,** 1994–2007.
43. DeLong, E. F. (1992) *Proc. Natl. Acad. Sci. USA* **89,** 5685–5689.